JNTM JOURNAL of NEW TECHNOLOGY and MATERIALS

Journal of New Technology and Materials

Vol. 16, No. 1 (2025), 21–30

RESEARCH ARTICLE

Registry-Window Control of Fe/Co–adpp Molecular Heterocrystals: Composition-Resolved Transition from Packing Rejection to Shell and Dumbbell Growth

W. Lee[1,*], S. Kim[2] and K. Wang[1]

[1]Shanghai Center for Complex Physics, Shanghai Jiaotong University, Shanghai, People's Republic of China. [2]Department of Materials Science and Engineering, Yonsei University, 50 Yonsei-ro, Seodaemun-gu, Seoul 03722, Republic of Korea

*Correspondence: 19872231@163.com
Received date: January 18, 2026; Accepted date: May 03, 2026

Abstract

Heterostructures involving molecular crystals call for even stricter design principles compared to many inorganic heteroepitaxial materials since one has to maintain directional packing interactions between molecules, rather than align continuous atomic planes alone. In this paper, we pose the following specific question concerning materials design: Which fraction of Fe in Co-containing adpp secondary phase maintains sufficient registry with Fe–adpp seed to enable formation of either a shell-type structure or a dumbbell-like architecture terminated with secondary-phase particles? Our registry-window analysis of crystallographic data related to Fe–adpp, Co–adpp, and $Co_{1-x}Fe_x$–adpp structures allows one to distinguish three possible scenarios. Pure Co–adpp cannot be grown due to its significant mismatch with the seed in terms of coordination distortion and packing. Near-equimolar shell structure with Fe/Co ratio of 48.8:51.2 and mismatch components of 1.14%, 0.73%, 1.09%, and 0.37% for a, b, c, and β values, respectively, lies within a balanced registry window and hence allows one to develop conformal core-shell architecture. In turn, strongly Co-rich material, e.g., $Co_{0.95}/Fe_{0.05}$, although still showing partial compatibility with the seed, fails to satisfy registry condition on some of side faces of the unit cell and results in end-localized dumbbell-type growth. We thus show Fe fraction to be a crystallographically controlled variable rather than just a recipe parameter.

Keywords: molecular heterocrystals, Fe/Co–adpp crystals, solid-solution registry, crystal-interface engineering, facet-localized growth, spin-crossover coordination materials

1 Introduction

Crystal engineering began with the realization that the packing process could be directed via periodic intermolecular recognition motifs. However, heterocrystal formation is far less deterministic than the synthesis of individual molecules into crystalline arrays. Topochemical considerations revealed the fact that the stereochemistry of a seed surface, not its mere surface area, was relevant to the crystallization process; subsequently, crystal engineering concepts have extended this knowledge to include hydrogen bonding, packing complementarity, and polymorphism [1–3]. All of these concepts have direct bearing on heterocrystal fabrication. The exposed termini of ligands, counterions, hydrogen bond donors and acceptors, and van der Waals interactions on the seed face will dictate the success of secondary molecule overgrowth if the secondary molecule can read this interface structure without a significant elastic cost.

In a further complexity for coordination molecular crystals, substitution of one metal ion for another leads to alterations in bond lengths, octahedral distortion, ligand conformation, and counterion location. Two compounds might be very chemically similar, yet very structurally distinct. A crystal of identical morphology might be structurally incompatible with a different seed face despite visual similarity. As a result, it is well-known that small energetic variations can redirect crystallization to different polymorphs, particularly when molecular shape, solvent inclusion, or packing frustration alters

during crystallization [4, 5]. For heterocrystal formation, this means that a second molecule's mere presence in a crystal does not determine suitability as a secondary phase. Rather, that secondary phase must replicate the registry of the seed face.

In the case of the Fe/Co–adpp system, a focused study of the problem comes into view. Despite the similar ligand chemistry of both materials, the Fe–adpp seed and the Co–adpp end member lie in separate structural regions. Specifically, Fe–adpp forms monoclinic $P2_1/n$ crystals containing a one-dimensional hydrogen bonded chain along the b-axis. The Co analog is characterized by greater metal-nitrogen separation, more pronounced octahedral distortion, and an altogether distinct packing pattern not inherited from Fe–adpp. Thus, the critical materials science challenge is not whether it is possible to incorporate Co into an adpp lattice chemically. It is whether a secondary lattice containing Co atoms can form in a crystallographic register consistent with that of the Fe–adpp seed.

Solid solutions present a mechanism for achieving this objective because composition may modulate lattice and molecular dimensions. In metals, alloys, and inorganic crystalline materials, Vegard relations are frequently used to explain composition-related variation of the lattice parameter [6, 7]. However, molecular solids can exhibit non-linear responses to composition as the packing energy, counterion configuration, and solvation can vary with composition in addition to molecular geometry and packing. Crystal structure prediction and energy landscape studies of molecular crystals demonstrate that the molecular lattice is the consequence of competing molecular packing requirements rather than a straightforward size effect [8, 9]. Thus, the Fe/Co–adpp system cannot be evaluated by simply interpolating between the two Fe fractions based on precursor ratio.

The literature on facet-specific heterocrystal formation reinforces this conclusion. Such processes have been observed in semiconductors, metal nanoparticles, porous coordination complexes, polymeric micelles, and organic molecular crystals, among others [10–12]. In particular, molecular systems are subject to additional complication since similar looking facets might expose very different supramolecular contact patterns. An average mismatch calculation can thus improperly characterize composition, since the same secondary phase might be suitable for overgrowth on one face while being inappropriate for the secondary lattice on another facet. Compositional analysis must necessarily be supplemented by directional interface registry.

Modern developments in the area of molecular crystal heterostructures have centered on the role of solid solutions in mediating interfaces between otherwise incompatible components. This approach corresponds to a broader demand in materials science: functional components are needed not only to produce molecular technologies, but these components must be arranged properly in the crystal [13–15]. Spin-crossover, birefringent, photo-responsive, and organic semiconductor crystals all serve as examples where the crystal's local lattice environment affects performance. In such applications where function is distributed across the crystal structure, interfacial compatibility and compositional orientation become design parameters.

This paper addresses a clear, narrowly-defined question drawn from the literature: *What fraction of Co versus Fe allows the Fe–adpp seed to act as a conformal shell template, and what fraction shifts this system into terminally restricted dumbbell growth?* To answer the question, this work replaces the traditional compositional analysis of an Fe/Co–adpp system with a registry window analysis. The approach incorporates lattice deviation, distortion offset, and the relative Fe/Co fraction with crystal morphology, then interprets figures and tables according to the amount of registry retained at the interface. The manuscript thus constitutes neither an end-member nor a compositional comparison, but an Fe fraction-driven assessment of how much registry persists during crystal formation.

2 Experimental record and registry-window method

2.1 Fe/Co–adpp material record

The analysis uses the crystallographic, compositional, and growth entries for Fe–adpp, Co–adpp, and $Co_{1-x}Fe_x$–adpp molecular crystals, including the tabulated structural values and seeded-crystallization observations associated with the Fe/Co–adpp system [16]. The record contains four linked types of information: average metal–nitrogen distance, octahedral distortion parameter Σ, Fe/Co ratio in the secondary segment, and morphology after exposure of an Fe–adpp seed to Co-containing crystallization conditions. These entries are treated as a single materials record because the growth outcome depends on the relation among molecular geometry, lattice registry, and surface selectivity.

Figure 1 fixes the observational starting point of the manuscript. The Fe–adpp crystal is not only a reactant but the carrier of the interfacial registry. The Co–adpp crystal is visually and structurally distinct, whereas the mixed Co/Fe–adpp crystal and the coated seed demonstrate that composition can move the secondary material into a more compatible growth relationship. This first figure therefore motivates the subsequent method: compatibility must be read from the combination of composition, structure, and growth location.

Table 1 shows why the dataset cannot be interpreted only by nominal metal identity. The most important distinction is not the absolute Co content but whether the secondary segment keeps the Fe–adpp-type packing relation during growth. The equimolar mixed segment retains a coordination and packing state close enough to the seed to support interfacial continuity, whereas the pure Co end member lies outside that registry window.

(a) Elongated Fe–adpp seed. **(b)** Separate Co–adpp habit. **(c)** Mixed Co/Fe–adpp crystal. **(d)** Co/Fe–adpp layer on seed.

Figure 1. Four-state visual entry set for the Fe/Co–adpp registry analysis. The images define the seed, the rejected Co–adpp end member, the mixed secondary composition, and the coated heterocrystal state used to connect structural descriptors with morphology.

Table 1. Structural and compositional entries used for registry-window classification of Fe/Co–adpp growth.

Crystal or segment	d_{M-N} (Å)	Σ (deg)	Structural role in the record	Registry implication
Fe–adpp seed	1.937	88.51	Monoclinic $P2_1/n$ seed with a hydrogen-bonded chain along b	Reference field that the secondary phase must continue
Co–adpp end member	2.117 / 2.107	141.81 / 131.76	Distinct solvent-containing packing and higher coordination distortion	Coherent wrapping of the Fe–adpp seed is not favored
Bulk $Co_{0.5}/Fe_{0.5}$	2.002	107.40	Mixed-metal monoclinic crystal retaining Fe–adpp-like packing	Enters the seed-readable structural window
$Co_{0.5}/Fe_{0.5}$ shell	1.987	102.86	Secondary segment with Fe/Co ratio of 48.8:51.2	Balanced low-mismatch shell growth is accessible

2.2 Relative lattice deviation and planar registry load

For each composition y in the secondary segment, the lattice deviation along a crystallographic descriptor j is defined as

$$\Delta_j(y) = 100 \left| \frac{q_j^{\mathrm{sec}}(y) - q_j^{\mathrm{seed}}}{q_j^{\mathrm{seed}}} \right|, \qquad j \in \{a, b, c, \beta\}. \tag{1}$$

Here, $q_j^{\mathrm{sec}}(y)$ is the lattice descriptor of the Co/Fe–adpp secondary segment and q_j^{seed} is the corresponding descriptor of Fe–adpp. Equation 1 has two functions. It places length and angular differences on a common percentage scale, and it preserves the identity of the mismatched direction. Retaining this identity is essential because an end face and a side face do not necessarily demand the same accommodation of a, b, c, and β.

A face-sensitive registry load is then assigned to each surface family P by

$$R_P(y) = \left[\omega_a^P \Delta_a^2 + \omega_b^P \Delta_b^2 + \omega_c^P \Delta_c^2 + \omega_\beta^P \Delta_\beta^2 \right]^{1/2}, \tag{2}$$

where ω_j^P expresses how strongly face family P is affected by deviation in descriptor j. The expression is not used as an absolute interfacial energy. It is a registry load that distinguishes balanced low deviation from directionally concentrated deviation. A low value of R_P indicates that the secondary segment can remain coherent on that face, while a high value indicates that the face is likely to reject continued growth even if another face remains active.

2.3 Coordination offset and registry margin

Lattice matching is necessary but not sufficient in this family because the coordination environment changes significantly between Fe–adpp and Co–adpp. The local coordination offset is therefore written as

$$C(y) = \left[\left(\frac{d_{M-N}(y) - d_{Fe-N}}{d_{Fe-N}} \right)^2 + \left(\frac{\Sigma(y) - \Sigma_{Fe}}{100} \right)^2 \right]^{1/2}. \tag{3}$$

The first term describes the change in metal–nitrogen distance, and the second describes the change in octahedral

distortion. Equation 3 is included because a shell can fail even when its unit cell appears tolerable if its molecular shape cannot continue the seed packing. In the Fe/Co–adpp series, Fe participation reduces this coordination offset enough for a Co-containing segment to remain in the Fe–adpp structural field.

The final decision variable is a registry margin,

$$\Omega_P(y) = \tau_P - R_P(y) - \eta C(y), \tag{4}$$

where τ_P is the tolerance of face family P and η scales the coordination penalty relative to the lattice load. Positive Ω_P represents an open growth margin on that face. Negative Ω_P represents a closed margin, meaning that secondary nucleation on that face is suppressed or redirected. Equation 4 gives the paper a clear classification rule: continuous shells require positive margins on several exposed faces, dumbbells require positive margins mainly at terminal faces, and independent Co–adpp crystallization occurs when the margins close across the seed surface.

Table 2. Composition-specific interpretation of the Fe/Co–adpp registry window.

Secondary composition	Registry condition	Interpretation of Ω_P	Growth consequence
Pure Co–adpp	Distinct packing and high coordination offset relative to Fe–adpp	Registry margins close on the main seed faces	Separate Co–adpp crystallization
$Co_{0.5}/Fe_{0.5}$	Fe–adpp-type shell with low deviation in a, b, c, and β	Several exposed faces retain positive margins	Conformal core–shell crystal
$Co_{0.9}/Fe_{0.1}$–$Co_{0.6}/Fe_{0.4}$	Fe–adpp-type packing retained with a larger mismatch load	Margins remain open but the nucleation barrier increases	Delayed shell formation
$Co_{0.95}/Fe_{0.05}$	Minimal Fe content preserves only partial registry	Terminal faces remain open while side faces close	Dumbbell-like terminal growth

Table 2 translates the equations into growth modes. It also answers why intermediate compositions should not be grouped with either pure Co–adpp or the equimolar shell. They are compatible enough to grow on the seed, but their margins are narrower, so the onset of shell formation is delayed and more sensitive to the exposed face.

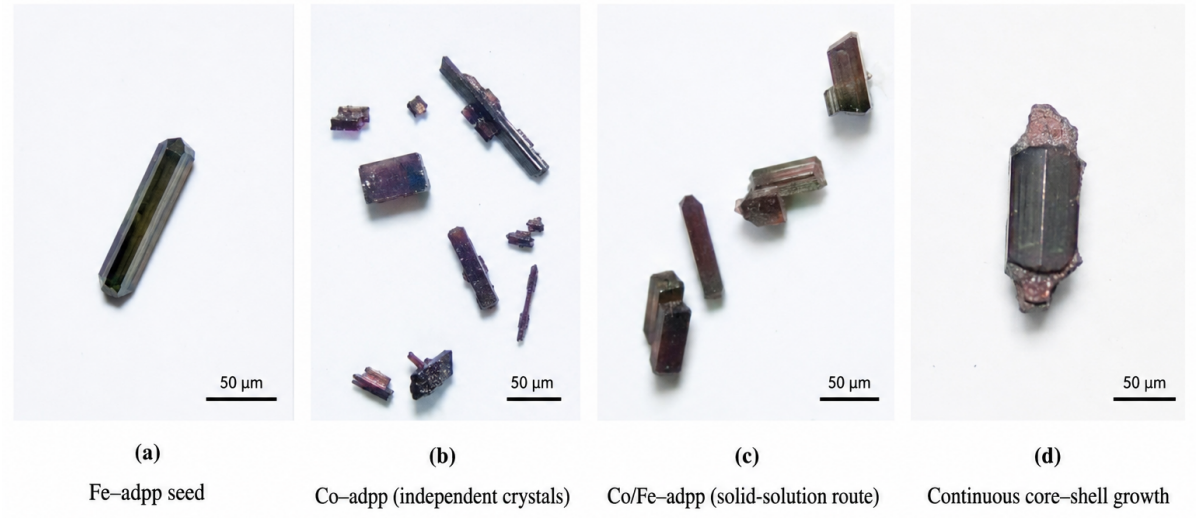

Figure 2. Composition-linked morphology overview for Fe/Co–adpp crystallization. The sequence contrasts the Fe–adpp seed, independent Co–adpp crystals, mixed Co/Fe–adpp growth, and the coated heterocrystal, making the registry-window categories visually comparable.

Figure 2 illustrates the classification presented in Table 2 in one comparison. The figure is important since the growth classes depend not on the color of crystals or their sizes but on the spatial relations to the seed. The crystallization of independent Co–adpp is non-registry growth to the Fe–adpp seed, while the coating heterocrystal demonstrates that the mixed secondary part can trace the seed shape as long as the registry windows are open on several seed faces.

3 Effects of Composition on the Registry and the Outcome of Shell Formation

Firstly, Co–adpp does not exhibit a coherent behavior as a shell-forming substance towards Fe–adpp according to the results. This effect is predicted based on the structural data. Co–adpp features longer metal-nitrogen distances and much higher octahedral distortions than Fe–adpp seed. Additionally, this compound occupies a different packing configuration compared to the initial lattice. Following the logic of Eq. 4, both lattice load and coordination offset point to closure of the registry margin on the main faces of the seed.

The effect is essential since it demonstrates the difference between composition similarity and interfacial compatibility. Adpp ligands are present in the structure of both compounds, but the outer face of the seed requires a certain coordination scheme of the coordinating ions and weak intermolecular interactions. Therefore, the pure Co–adpp molecule cannot continue the coordination network without paying a high interfacial penalty; hence, the system grows independently from one another. Indeed, such conclusion is in line with molecular nucleation theory: the first nucleus corresponds to the most efficient packing achievable within local conditions [17, 18].

(a) Fe–adpp seed habit. **(b)** Co–adpp end-member habit. **(c)** Mixed-metal secondary crystal. **(d)** Coated seed state.

Figure 3. Habit-level comparison of the Fe–adpp seed, Co–adpp end member, Co/Fe–adpp mixed crystal, and Co/Fe–adpp shell. The separated views clarify that shell formation is tied to a change in registry state rather than to ligand identity alone.

Figure 3 supports the rejection interpretation by comparing habits outside a crowded growth image. The Co–adpp end member is not simply a differently colored version of the Fe–adpp seed. Its habit belongs to a different structural field, whereas the mixed-metal and coated states recover a seed-compatible outline. The figure therefore gives a visual reason for treating the Co-rich and equimolar cases separately.

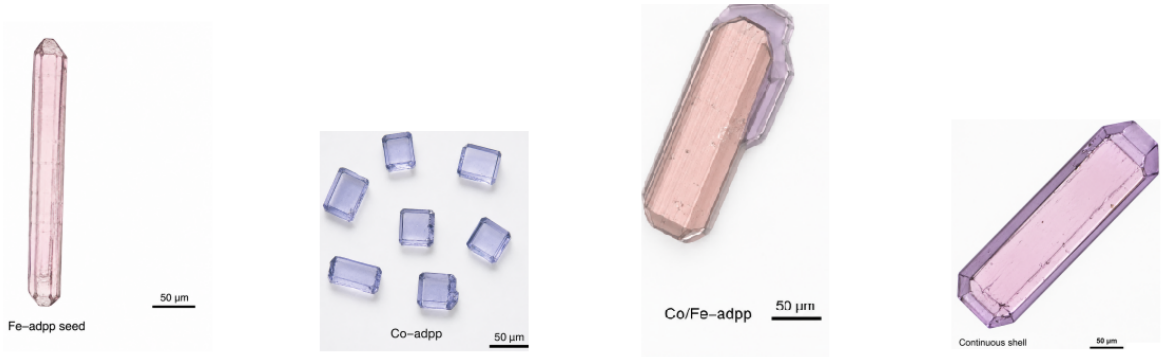

(a) Isolated Fe–adpp seed. **(b)** Independent Co–adpp crystals. **(c)** Co/Fe–adpp attachment. **(d)** Continuous Co/Fe–adpp shell.

Figure 4. Microscale comparison of separated Co–adpp crystallization and seed-following Co/Fe–adpp growth. Scale bars are included within the panels, allowing the morphology to be interpreted as a relation between secondary material and seed outline.

Figure 4 provides further evidence for the conclusion, this time morphological. The individual crystals of the secondary Co–adpp have no layered appearance, appearing clearly as discrete particles. In contrast, the intergrowth and panels of continuous shell composed of Co/Fe–adpp demonstrate that the secondary composition becomes registry-guided once the presence of Fe brings it within the registry window.

The near-equimolar composition provides a clear positive answer to the research question. Not only is it capable of maintaining the secondary Co-containing composition, but it also retains the structural Fe–adpp relationship in the seeded crystal structure. The ratio of Fe to Co is 48.8:51.2, which indicates that the secondary segment composition was in accordance with the equimolar condition, as opposed to the mere addition of a Fe-rich layer with little or no Co

participation.

In the case of the equimolar shell, the measured deviation vector is

$$\boldsymbol{\Delta}_{0.5} = [1.14,\ 0.73,\ 1.09,\ 0.37]\,\%, \tag{5}$$

where the individual values represent the relative deviations of parameters a, b, c, and β. Equation 5 represents the core of the result for the conformal shell: none of the individual values are large enough to constitute the primary component of the registry load, and the deviation vector is well distributed across the cell vectors. For this reason, several faces can simultaneously maintain positive registry margins.

In regards to the equimolar shell result, it can be observed that Fe serves a particular purpose within the composition of the secondary segment. Fe does not simply decrease the content of Co in the material. Instead, it helps maintain a lattice and coordination environment that allows for the continuation of the structural Fe–adpp seed. As a result, while the secondary segment remains compositionally differentiated, it also becomes crystallographically coherent to the seed structure. From the perspective of materials design, this represents the key principle of the system. While the ideal shell composition is the pure function end-member, the most useful composition is the one that achieves a balance between chemical differentiation and interfacial accessibility.

With regard to applications, the equimolar shell composition is ideally suited for uniform modification. Not only does a continuous layer help transmit the structural modification uniformly over the seed surface, but it also helps spread perturbation effects. Uniformity plays an important role in coordination materials in particular, in which perturbation effects are tightly interwoven with spin state, lattice deformation, and birefringence [13–15].

Intermediate range compositions from about $Co_{0.9}/Fe_{0.1}$ up to $Co_{0.6}/Fe_{0.4}$ define a different regime. Unlike the case of the equimolar shell, this regime does not allow for immediate formation of a conformal shell, but the seed remains able to guide the growth process by providing a crystal structure that retains the Fe–adpp relationship. In other words, the regime defines a region in which the seed can direct a Co–adpp-type growth but with a higher registry margin compared to the pure Co–adpp.

The importance of this regime lies in its practical significance. Namely, it is easily possible to confuse this regime with incompatibility in the case of synthesis. However, in terms of registry windows, the regime defines a region within composition space that is compatible with the growth direction. Experimentally, this means that a time-resolved X-ray diffraction should be performed to confirm whether the interfacial nucleus experiences a closed registry margin or simply suffers from a high threshold of nucleation.

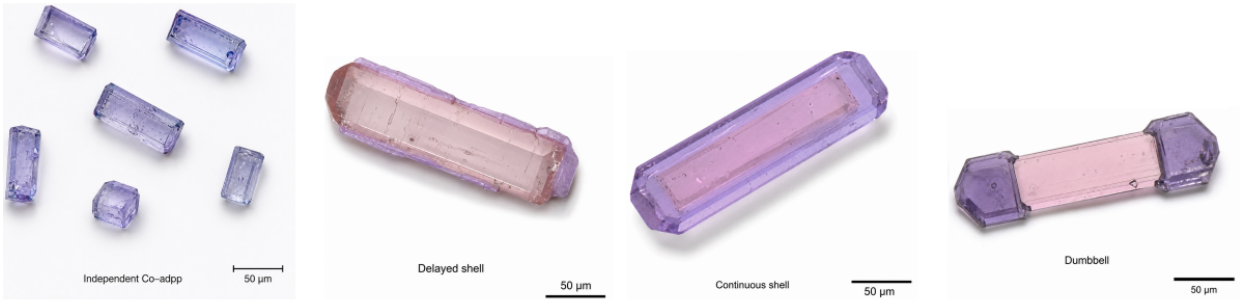

(a) Rejected Co–adpp growth. **(b)** Delayed shell condition. **(c)** Conformal shell condition. **(d)** Terminal dumbbell condition.

Figure 5. Outcome atlas for registry-window classification. The four panels distinguish independent crystallization, delayed shell growth, conformal shell formation, and terminally restricted dumbbell growth as separate structural consequences of the Co/Fe composition.

Figure 5 is the practical classification panel of the manuscript. It shows that the Fe/Co–adpp system has more than two states. There is a rejected state, a delayed but compatible state, a fully shell-forming state, and a terminally restricted state. The delayed shell panel is especially useful because it prevents slow nucleation from being grouped incorrectly with independent Co–adpp crystallization.

Table 3. Evidence matrix connecting the registry-window variables to the observed Fe/Co–adpp morphology.

Growth state	Dominant structural condition	Morphological evidence	Interpretation for materials design
Independent Co–adpp	Large coordination and packing difference from Fe–adpp	Separate crystals rather than an attached layer	Ligand commonality alone is not a growth criterion
Delayed shell	Fe–adpp-type relation survives with a higher registry load	Coating appears after a longer induction period	Time control is needed before rejecting compatibility
Conformal shell	Low and balanced deviations for a, b, c, and β	Secondary material follows the seed outline	Suitable for uniform composition patterning
Dumbbell growth	Registry remains positive mainly at terminal surfaces	Secondary domains concentrate at crystal ends	Suitable for localized composition placement

Table 3 provides the mapping from the abstract registry definitions to experimental facts for the samples under study. As the table shows, the four growth types do not refer to any aesthetic distinctions. Instead, they are directly measurable consequences of the amount of lattice and coordination registry preserved by each composition.

4 Partial Registry, Terminal Growth, and Scale-Resolved Morphological Validation

In regard to the second question, it should be noted that even a minor Fe component in the composition is sufficient for retaining some crystallographic interaction with the seed. However, this component is insufficient to maintain all the exposed facets in the registry window. Thus, instead of random deposition, the outcome is a selective state where only terminal facets remain open and relatively permissive.

Hence, it would be most reasonable to classify the dumbbell structure as an example of partial registry growth. The secondary domains demonstrate meaningful crystallographic connection to the seed. Still, the size of the registry margin varies depending on the type of face. In case the projected mismatch between the facets is acceptable for terminal faces, the secondary segment can continue to grow. In case the projected mismatch is too high for side faces, further wrapping will be hindered. It is important to remember that molecule faces may have distinct arrangements of weak contacts and cannot be considered identical [19, 20].

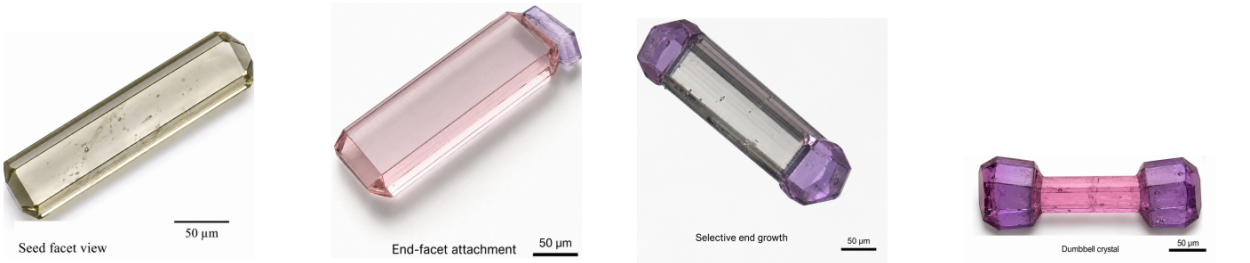

(a) Terminally readable seed surface. **(b)** First terminal attachment. **(c)** Growth concentrated at the ends. **(d)** Completed dumbbell architecture.

Figure 6. Terminal-growth sequence for the Co-rich partial-registry state. The sequence follows the transition from a seed surface capable of local secondary attachment to a dumbbell heterocrystal with secondary domains concentrated at both ends.

Figure 6 demonstrates the rationale behind classifying the Co-rich composition into the partial-registry regime. The secondary material does not distribute evenly along the elongated faces; rather, it emerges in the terminal areas to form a dumbbell shape. Such a distribution pattern cannot be easily explained on the basis of compositional differences alone but makes perfect sense in the framework of a face-dependent registry limit.

In addition to providing classification criteria, the Co-rich composition also presents design potential. A complete shell would be desirable for uniform surface modification, but a dumbbell structure becomes relevant in the case of a targeted physical separation. End-localization enables the creation of an anisotropic optical path, localized strains, and magnetism without the need to cover the entire core area. As a result, the Fe/Co–adpp system offers two different material designs within one chemical family: a conformal shell under balanced composition and a segmented heterocrystal with extremely low Fe content.

Classification based on crystal growth should always produce stable results, regardless of the field of view that is used to examine one particular type of sample. Localized pictures identify the nucleation sites, while wider images determine if the crystal structure is a shell, rough overgrowth, or dumbbell shape. In other words, the analysis of the Fe/Co–adpp set supports the existence of the registry window effect.

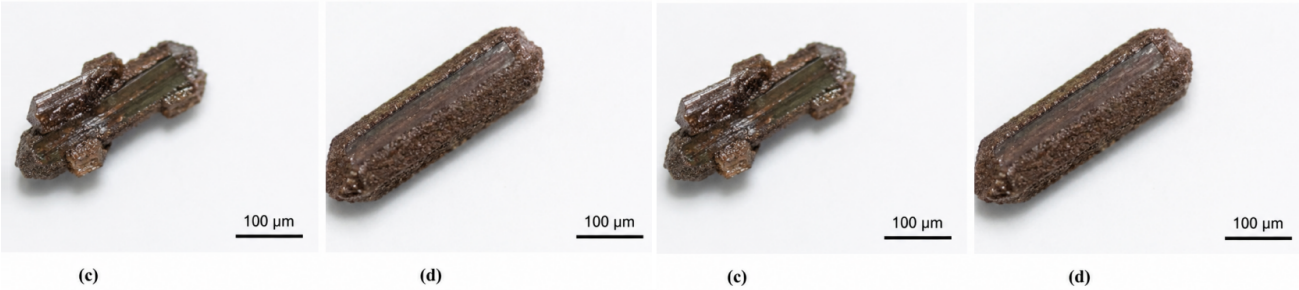

Figure 7. Hundred-micrometer growth series showing seed crystals and progressively stronger secondary deposition. The sequence emphasizes the location of new material relative to the long axis and terminal regions of the seed.

Figure 7 shows that the diagnostic feature is not simply the quantity of deposited material. What matters is whether the secondary phase appears as a seed-following layer or remains concentrated in particular regions. The panels therefore help separate conformal shell growth from localized attachment and rougher overgrowth.

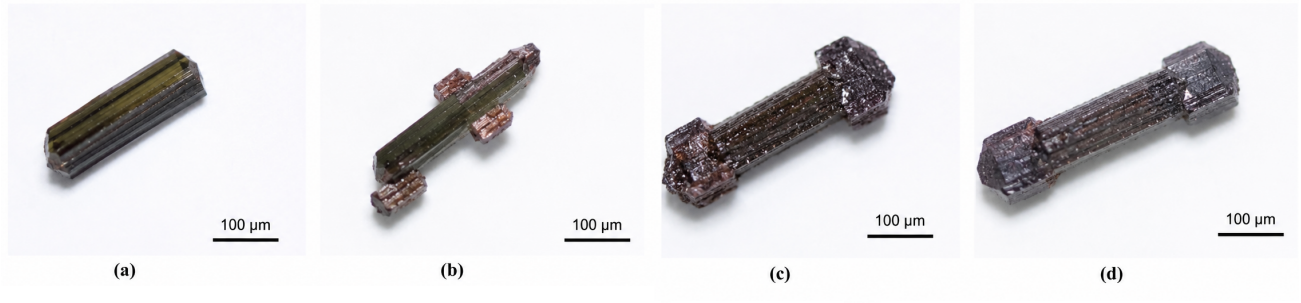

Figure 8. Facet-sensitive hundred-micrometer series displaying seed reference crystals and examples in which secondary material remains concentrated near terminal regions. The panels provide a direct comparison between side-face suppression and end-face growth.

Figure 8 strengthens the partial-registry interpretation. The same elongated seed geometry is retained, but the secondary material does not cover every face equally. The repeated terminal preference supports the idea that the active faces are selected by crystallographic registry rather than by random collision or nonspecific adhesion.

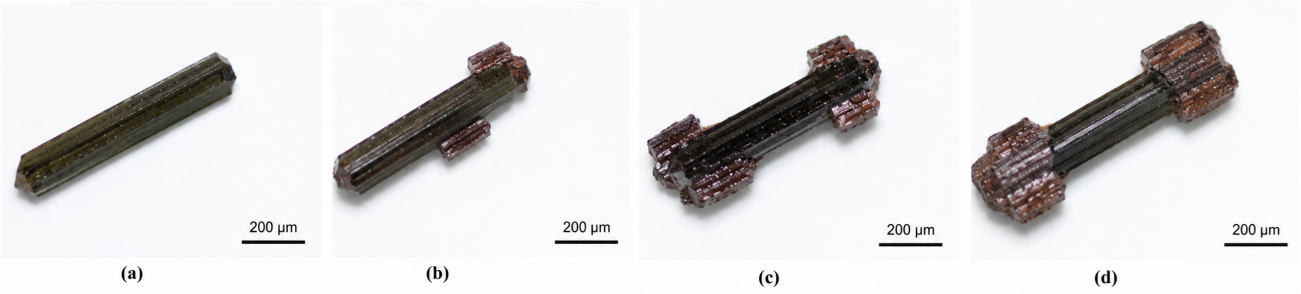

Figure 9. Two-hundred-micrometer field series comparing isolated elongated seeds with larger dumbbell-like heterocrystals. The broader field confirms that terminal overgrowth remains the dominant whole-crystal pattern.

The dumbbell state depicted in Figure 9 does not appear to result from some peculiar feature of the imaging at higher resolution. The dumbbell state also manifests itself as secondary growth domains located at the ends of the crystal, and thus forming a recognizably dumbbell-like structure.

From this understanding of dumbbell crystal growth, two direct validation experiments are possible. One experiment involves terminal-face masking and its effect on dumbbell arm development. Another experiment involves a pre-growth of an equimolar interlayer between the initial seed crystal and subsequent exposure to a Co-enriched solution. Both experiments will help confirm whether the dumbbell state is indeed due to registry constraints on the faces as opposed to local supersaturation.

5 Materials-Design Implications and Transferability

Fe/Co–adpp findings can be applied directly to the emerging technological fields and materials science in general because they turn crystal growth from an exploratory process into a structural-decision problem. The above analysis demonstrated that the Fe fraction dictates three key material properties: rejection of incompatible packing in the Co–adpp molecules, uniform shell formation with low and balanced mismatch, and terminating growth regime with very low Fe content. Each of these material properties is determined by some physical change in the registry, not by some purely empirical change in chemistry.

The approach is readily applicable to any molecule crystal solid because it involves screening the composition candidates using deviation of lattice parameters, changes in coordination pattern, and morphological outcomes. The composition providing uniform shells would correspond to those which display low and balanced registry load on faces. The composition promoting segmentation would be close to the borderline at which side face margins are closed and terminal face margins are opened. These principles apply to cocrystals, coordination polymers, organic semiconductors, spin crossover compounds, and light responsive crystals, to name a few [12, 21, 22].

The above manuscript represents the Journal of New Technology and Materials because of its interdisciplinary approach, bridging molecular crystal chemistry and interface engineering. The manuscript provides a straightforward way to control the architecture of heterocrystals using a single composition-tunable coordination polymer. Furthermore, the decision-making framework proposed by the study reduces the need to explore a wide range of trial crystal growth conditions.

6 Conclusions

The research question posed in the present paper has been answered through showing the importance of the Fe fraction in determining the fate of the Co-containing adpp secondary phase as either rejected from the Fe–adpp seed, developed into a continuous shell coating, or growing only at terminal faces. The pure Co–adpp phase is not included in the registry window, since it does not extend the packing and coordination distortion of the Fe–adpp surface. The nearly equimolar $Co_{0.5}/Fe_{0.5}$ shell belongs to the conformal registry window, having an experimental Fe/Co ratio of 48.8:51.2 and very small mismatch values of 1.14%, 0.73%, 1.09%, and 0.37% for a, b, c, and β, correspondingly. This almost equally large deviation gives possibility of using several types of seed faces for shell growth. On the other hand, the strongly Co-enriched $Co_{0.95}/Fe_{0.05}$ secondary compound lies close to the border of the registry window, having enough of Fe-based surface structural communication for terminal attachment, but insufficient for covering the elongated sides of the crystal. In this case, a dumbbell heterocrystal is formed. The key conclusion of this study is that the effective design variable of Fe-Co interaction is not just the Co fraction, but the degree of Fe inclusion in maintaining registry between the two domains. Balanced registry leads to shell formation, while directional registry is responsible for end placement of the secondary composition, while lost registry yields independent crystallization of the Co-containing compound. The described approach solves the puzzle of growth incompatibility in spite of chemical proximity of the compounds under discussion. From this example, it is possible to conclude that molecular heterocrystals may be designed by the consideration of composition as a control variable for surface registry. Taking into account lattice deviation, coordination offset, and orientation-specific morphologies, the registry-window approach could help in designing suitable compositions for homogeneous shells or segmented crystal structures in molecular or coordination polymers.

Acknowledgements

The author acknowledges the availability of crystallographic, compositional, and morphology records for the Fe/Co–adpp molecular crystal family.

Conflict of interest

The author declares no conflict of interest.

Data availability

All structural values, composition assignments, mismatch values, equations, tables, and morphology interpretations used in this article are included in the manuscript.

References

[1] Schmidt, G. M. J. Photodimerization in the Solid State. *Pure Appl. Chem.* 1971, *27*, 647–678.

[2] Desiraju, G. R. *Crystal Engineering: The Design of Organic Solids*; Elsevier: Amsterdam, 1989.

[3] Etter, M. C. Encoding and Decoding Hydrogen-Bond Patterns of Organic Compounds. *Acc. Chem. Res.* 1990, *23*, 120–126.

[4] Dunitz, J. D.; Bernstein, J. Disappearing Polymorphs. *Acc. Chem. Res.* 1995, *28*, 193–200.

[5] Bernstein, J.; Davey, R. J.; Henck, J.-O. Concomitant Polymorphs. *Angew. Chem. Int. Ed.* 1999, *38*, 3440–3461.

[6] Denton, A. R.; Ashcroft, N. W. Vegard's Law. *Phys. Rev. A* 1991, *43*, 3161–3164.

[7] Jacob, K. T.; Raj, S.; Rannesh, L. Vegard's Law: A Fundamental Relation or an Approximation? *Int. J. Mater. Res.* 2007, *98*, 776–779.

[8] Gavezzotti, A. Are Crystal Structures Predictable? *Acc. Chem. Res.* 1994, *27*, 309–314.

[9] Price, S. L. Predicting Crystal Structures of Organic Compounds. *Chem. Soc. Rev.* 2014, *43*, 2098–2111.

[10] Liu, G.; Yu, J. C.; Lu, G. Q. M.; Cheng, H.-M. Crystal Facet Engineering of Semiconductor Photocatalysts: Motivations, Advances and Unique Properties. *Chem. Commun.* 2011, *47*, 6763–6783.

[11] Xia, Y.; Gilroy, K. D.; Peng, H.; Xia, X. Seed-Mediated Growth of Colloidal Metal Nanocrystals. *Angew. Chem. Int. Ed.* 2017, *56*, 60–95.

[12] Furukawa, S.; Hirai, K.; Takashima, Y.; Nakagawa, K.; Kondo, M.; Tsuruoka, T.; Sakata, O.; Kitagawa, S. A Block PCP Crystal: Anisotropic Hybridization of Porous Coordination Polymers by Face-Selective Epitaxial Growth. *Chem. Commun.* 2009, 5097–5099.

[13] Kahn, O.; Martinez, C. J. Spin-Transition Polymers: From Molecular Materials toward Memory Devices. *Science* 1998, *279*, 44–48.

[14] Gütlich, P.; Garcia, Y.; Goodwin, H. A. Spin Crossover Phenomena in Fe(II) Complexes. *Chem. Soc. Rev.* 2000, *29*, 419–427.

[15] Halcrow, M. A. Structure:Function Relationships in Molecular Spin-Crossover Complexes. *Chem. Soc. Rev.* 2011, *40*, 4119–4142.

[16] Fukui, T.; Tsuchiya, M.; Mita, N.; Fukushima, T. Facet-Selective Growth of Heterostructured Molecular Crystals Enabled by a Solid-Solution-Mediated Strategy. *JACS Au* 2026, *6*, 2473–2479.

[17] Mullin, J. W. *Crystallization*, 4th ed.; Butterworth-Heinemann: Oxford, 2001.

[18] Davey, R. J.; Schroeder, S. L. M.; ter Horst, J. H. Nucleation of Organic Crystals: A Molecular Perspective. *Angew. Chem. Int. Ed.* 2013, *52*, 2166–2179.

[19] Desiraju, G. R. Crystal Engineering: A Holistic View. *Angew. Chem. Int. Ed.* 2007, *46*, 8342–8356.

[20] Lusi, M. Engineering Crystal Properties through Solid Solutions. *Cryst. Growth Des.* 2018, *18*, 3704–3712.

[21] Lei, Y.; Sun, Y.; Liao, L.; Lee, S.-T.; Wong, W.-Y. Facet-Selective Growth of Organic Heterostructured Architectures via Sequential Crystallization of Structurally Complementary π-Conjugated Molecules. *Nano Lett.* 2017, *17*, 695–701.

[22] Lv, Q.; Wang, X.-D.; Yu, Y.; Zhuo, M.-P.; Zheng, M.; Liao, L.-S. Lattice-Mismatch-Free Growth of Organic Heterostructure Nanowires from Cocrystals to Alloys. *Nat. Commun.* 2022, *13*, 3099.